

Impact of the structure and reactivity of nickel particles on the catalytic growth of carbon nanofibers

Marjolein L. Toebes, Johannes H. Bitter, A. Jos van Dillen, Krijn P. de Jong*

Department of Inorganic Chemistry and Catalysis, Debye Institute, Utrecht University, PO Box 80 083, 3508 TB Utrecht, The Netherlands

Abstract

Catalytically grown fishbone carbon nanofibers (CNF), are prepared by the decomposition of carbon-containing gases (CH_4 , CO/H_2 or $\text{C}_2\text{H}_4/\text{H}_2$) over a silica-supported nickel catalyst and an unsupported nickel catalyst at 550°C . It turns out that both the nickel particle size and the nature of the carbon-containing gas significantly affects the CNF growth process. We demonstrate that at the chosen temperature small supported nickel particles need a carbon-containing gas with a relatively low reactivity, like CH_4 or CO/H_2 , to produce CNF. The resulting fishbone CNF have a uniform and small diameter (25 nm). The CNF thus synthesized hold great potential, e.g. as catalyst support material. However, the large unsupported nickel particles only produce CNF using a reactive carbon-containing gas, like $\text{C}_2\text{H}_4/\text{H}_2$. The CNF thus obtained show a variety of morphologies with a large range of diameters (50–500 nm). The CNF yield is a subtle interplay between the nickel particle size and consequently the exposed crystal planes on the one hand and the reactivity of the carbon-containing gas on the other. © 2002 Elsevier Science B.V. All rights reserved.

Keywords: Carbon nanofibers; Nickel catalyst; Catalytic growth

1. Introduction

Carbon nanofibers (CNF) have gained increasing attention in the last few years due to their high strength, chemical purity and chemical inertness which features make them ideally suitable for use as a catalyst support [1–3]. The two most encountered forms of CNF are the fishbone and the parallel type (also called multiwalled carbon nanotubes). In the fishbone type fibers the graphite planes are oriented at an angle to the central axis, thus exposing graphite edge sites. If the graphite planes are oriented parallel to the central axis, like in the parallel type of CNF, only basal graphitic planes are exposed.

Because CNF consist of carbon, a carbon-containing gas is needed for the synthesis of these materials. The production of reactive carbon intermediates from this carbon-containing gas is a crucial step in the synthesis procedure. This can be achieved by activation of graphite by laser vaporization [4], electric arc-discharge [5,6] or by the dissociation of a carbon-containing gas on the surface of a metal catalyst like Ni, Fe or Co [1–3,7–10]. The latter route, which is called catalytic synthesis, is the only technique with which one can produce very pure CNF in large quantities, while tuning of physico-chemical properties like surface structure, diameter and morphology is possible.

The relevance of carbon materials is clearly envisioned by their application as a support in various catalytic processes, especially selective hydrogenations. The catalytic performance of the carbon (graphite, activated carbon) supported catalysts can be tuned by a

* Corresponding author. Tel.: +31-30-2536762;
fax: +31-30-2511027.
E-mail address: k.p.dejong@chem.uu.nl (K.P. de Jong).

change of the features of the support, like the amount of oxygen-containing surface groups [11,12] the accessibility of the support [13,14] and the degree of carbon ordering [15]. We expect a similar influence of the support on the performance of a metal/CNF catalyst. However, the preparation of uniform CNF with defined properties, like diameter and macroscopic porosity, is not well understood. The most important parameters which influence these properties are the nature of the metallic catalyst particles and that of the carbon-containing gas [1,9,16–27]. Although effects of promoters has been described as well [28,29].

Variations in the choice of the metal and the growth temperature can alter the ordering of the graphite planes from parallel to fishbone [16,17]. Parallel CNF can be grown, especially using CO, from iron [16] and cobalt particles [18] as well as from nickel at elevated temperatures [19]. Fishbone fibers are mainly obtained when using nickel and nickel–iron alloy catalysts with methane as the carbon-containing gas [20–22].

As stated, the dissociation of a carbon-containing gas on a metal surface is a key step in the production of catalytically grown CNF. It is noted that the dissociation rate of carbon-containing gases is among other things dependent on the detailed surface structure of the metal thus influencing the CNF growth process [23–26]. For example, Ni(110) and (100) [23] surfaces are much more active for methane dissociation than the Ni(111) surface [25,26].

The particle size of the metal can affect the characteristics of the CNF as well. The diameter of the nanofibers is controlled by the size of the metal particles from which the nanofibers start to grow [1,9,16]. This allows us to tune the diameter of the CNF. Previous studies have revealed that CNF can be produced with surface areas of up to 300 m²/g [27], which is comparable to the surface areas commonly reported for selective hydrogenation catalysts [13].

Due to the diversity of the applied reaction conditions in the above-mentioned studies, it is not possible to directly compare the obtained results with respect to the tuning of the CNF. To our best knowledge no systematic study has been carried out on the influence of the metal particle size of the growth catalyst and the nature of the carbon-containing gas on the CNF growth and their physico-chemical properties, like diameter and textural properties.

In this paper, we present the results of our study on the catalytic decomposition of several carbon-containing gases (CH₄, CO/H₂ and C₂H₄/H₂) on a silica-supported nickel catalyst and on an unsupported nickel catalyst. It turns out that the combination of the nickel particle size and the nature of the carbon-containing gas significantly affects the CNF growth process. We demonstrate that small supported nickel particles need a carbon-containing gas with a relatively low reactivity, like CH₄ or CO/H₂, to produce CNF. The resulting fishbone CNF have a uniform and small diameter. However, the large unsupported nickel particles only produce CNF using a reactive carbon-containing gas, like C₂H₄/H₂. The CNF thus obtained show a variety of morphologies with a large range of diameters.

2. Experimental

2.1. Preparation of growth catalysts

Silica-supported nickel catalysts with a metal loading of 20 wt.% were prepared by deposition–precipitation using the hydrolysis of urea at 90 °C [30,31]. Silica (8.5 g, Degussa Aerosil 200) was suspended in 1 l of demi-water at 90 °C and mechanically stirred at 1000 rpm. Nickel nitrate hexahydrate (10.55 g, Acros 99%) was added and the pH was adjusted to 3–4 using nitric acid (Merck p.a.). Subsequently, 6.95 g urea (Acros p.a.) was introduced. After 16 h of reaction, the mixture was cooled to room temperature and filtered. The residue was washed three times with demi-water, followed by drying at 120 °C for 16 h. Finally, a sieve fraction of 425–850 μm of the catalyst precursor was calcined in static air at 600 °C (ramp 5 °C/min) for 3 h. The calcined samples were stored in static air for further use.

Unsupported nickel was synthesized from nickel carbonate, precipitated from a nickel nitrate solution using ammonium bicarbonate (Aldrich 99%) at room temperature and a pH of about 9.0. [22]. Nickel nitrate (24.77 g) was dissolved in 1 l demi-water and the solution was mechanically stirred at 1000 rpm. Subsequently solid ammonium bicarbonate (~25 g) was added until the supernatant was colorless. After filtering, the precipitate was treated likewise the supported catalyst, except that calcination was carried out at 500 °C.

2.2. CNF growth

A weighed sample (100 mg) of the nickel growth catalyst, loaded in a spherical quartz vessel with a porous quartz plate at the bottom, was reduced in a flow of 20% hydrogen in argon (flow rate 100 ml/min). The temperature was raised to 700 °C for Ni/SiO₂ (ramp 5 °C/min) and 500 °C for the unsupported Ni sample (ramp 5 °C/min) and kept at these levels for 2 h. After reduction the reactor was brought at the desired reaction temperature, maintaining 20% hydrogen in argon flow.

Subsequently, synthesis gas (20% CO, 7% H₂), methane (20% CH₄) or an ethene/hydrogen mixture (20% C₂H₄, 7% H₂) balanced with Ar was passed through the reactor for 10 h to grow CNF. The total flow was always 100 ml/min. After 10 h, the sample was cooled down to room temperature under an argon stream. During the growth, the conversion of the gases was assessed by gas chromatography analysis using an HP5890A gas chromatograph equipped with a 12 ft Porapack Q column. The following equation was used for the determination of the carbon deposition rate:

$$\text{rate} = \frac{(C_0 - C_{\text{offgas}} - C_{\text{by-products}}) \times 12.01}{g_{\text{Ni}}} \left(\frac{g_{\text{CNF}}}{g_{\text{Ni}}h} \right)$$

where C_0 is the feed rate of carbon (mol/h), C_{offgas} the rate of unconverted feed (mol/h), $C_{\text{by-products}}$ the rate of gaseous carbon-containing by-products formed during CNF growth (mol/h) and g_{Ni} the amount of nickel in grams used for the CNF growth. This results in a C-deposition rate expressed in gram carbon per gram nickel per hour.

To remove the growth catalyst, i.e. SiO₂ and not encapsulated nickel, from the CNF after the growth process, the fibers are subsequently refluxed in 1 M KOH solution and concentrated HCl for 1 h. After this treatment the sample was filtered, thoroughly washed with demi-water and dried in air at 120 °C.

2.3. Characterization

The growth catalysts and the produced fibers were examined in a Philips CM-200 FEG transmission electron microscope (TEM) operated at 200 kV. Samples were prepared by suspending the fibers in ethanol under ultrasonic vibration. Some drops of the thus produced suspension were brought onto a porous

carbon film on a copper grid. Scanning electron microscopy (SEM) was performed using a Philips XL30 FEG apparatus. Specific surface areas (BET) and pore volumes of the growth catalysts and the CNF were calculated from nitrogen physisorption data measured at –196 °C with a Micromeritics ASAP 2400 apparatus. Prior to the physisorption experiments the samples were evacuated at 200 °C for at least 16 h. XRD patterns were recorded at room temperature with a Nonius PDS 120 powder diffractometer system equipped with a position-sensitive detector with a 2θ range of 120° using Co K α_1 ($\lambda = 1.78897 \text{ \AA}$) radiation.

3. Results

Electron micrographs of both the growth catalysts used in this study are shown in Fig. 1. It can be clearly seen that the nickel particle size (the dark spots) in the Ni/SiO₂ catalyst is small (d , 5–10 nm) with a narrow size distribution. The unsupported nickel catalyst consists of micrometer-sized conglomerates of 50–1000 nm particles. The nickel particle sizes were also determined by XRD by an analysis of the line broadening of the Ni(1 1 1), (2 0 0), (2 2 0) and (3 1 1) reflections, see Fig. 2. The NiO phase observed with XRD is formed when the reduced nickel catalyst is exposed to air prior to the XRD measurement. This phase is not present while growing CNF. For the Ni/SiO₂ catalyst line broadening analysis of the Ni reflections leads to similar sizes as found with the TEM, which indicates that the nickel particles are small single crystals. On the other hand, for the unsupported Ni, XRD leads to $d > 50 \text{ nm}$. Probably small crystallites are also present because the peaks are slightly broadened at the bottom. The particles (50–1000 nm) as shown with SEM (Fig. 1) most likely are highly polycrystalline.

From both Ni catalysts, CNF were grown using different carbon-containing gases. The amounts of CNF grown in 10 h with these catalysts in the respective carbon-containing gases are shown in Fig. 3. It can be seen that over this period of time Ni/SiO₂ is most effective in growing CNF from CH₄ (18 g_{CNF}/g_{Ni}) and CO/H₂ (31 g_{CNF}/g_{Ni}) while unsupported Ni is most effective for CNF growth from C₂H₄/H₂ (20 g_{CNF}/g_{Ni}). Evidently the CNF yield depends on the combination of the type of nickel catalyst and the carbon-containing gas.

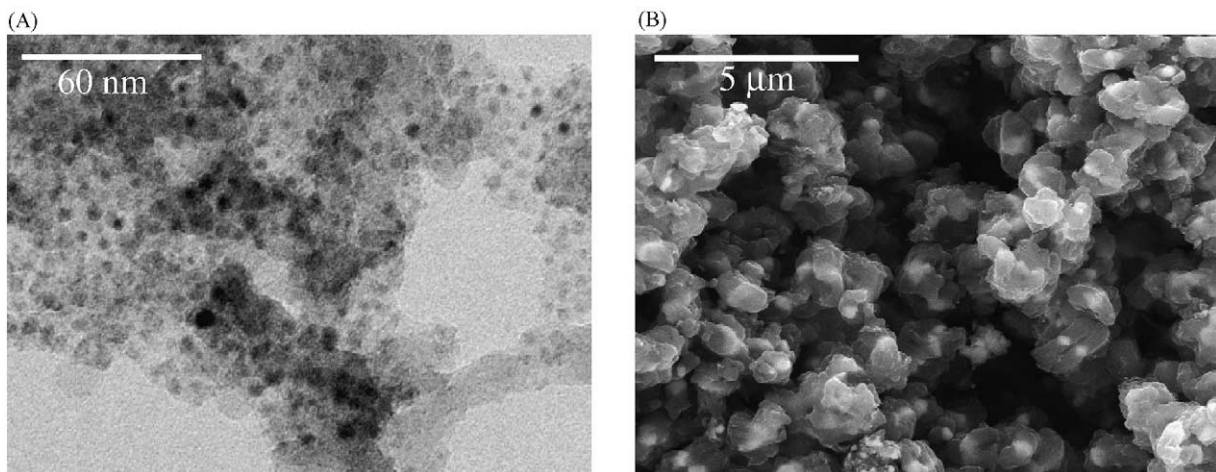


Fig. 1. (A) TEM micrograph of reduced Ni/SiO₂; (B) SEM micrograph of the reduced unsupported Ni catalyst.

To examine how this yield is brought about we monitored the course of the deposition in time. The results are summarized in Fig. 4. When CNF were grown with the use of Ni/SiO₂ from CH₄ and CO/H₂, the carbon deposition rate increased somewhat and reached a steady state which leads to a high yield after 10 h. When, however, C₂H₄/H₂ was used a high initial deposition rate was observed which dropped rapidly to zero already within 30 min. Obviously, the catalyst deactivated completely. With the unsupported Ni catalyst

the situation is rather different. With CH₄ and CO/H₂ low initial conversions were measured. These conversions diminished fast, which explains the negligible yields, even after 10 h on stream. The unsupported catalyst turned out to be more active and the activity more stable with C₂H₄/H₂, however, also in this case the catalyst deactivated completely albeit at a lower rate. The apparently high yield, as shown in Fig. 3B had already been attained within the first period of 3 h.

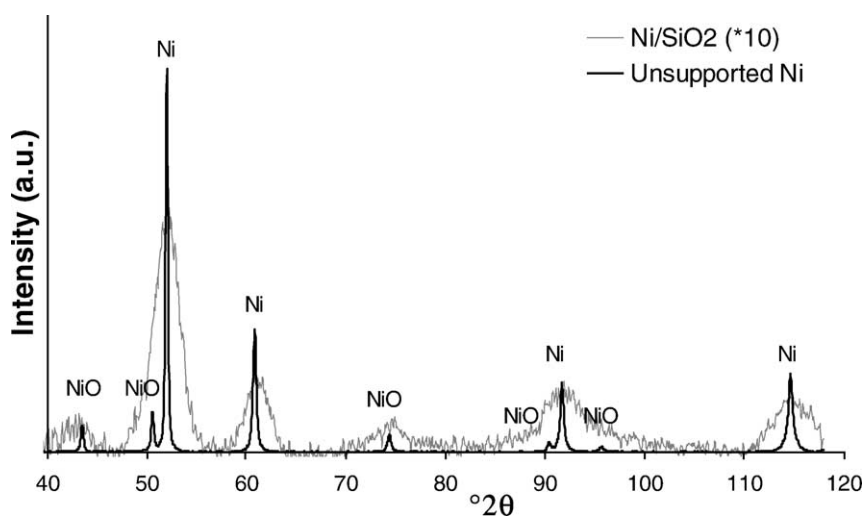


Fig. 2. XRD patterns of reduced Ni/SiO₂ and of the reduced unsupported Ni catalyst.

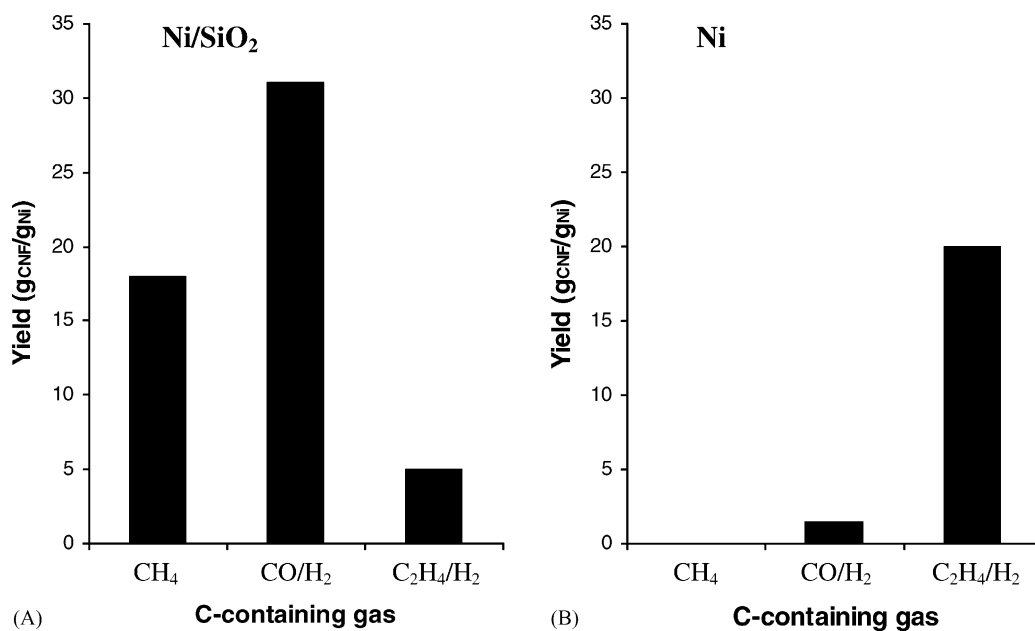


Fig. 3. Yield of CNF as a function of the carbon source used: (A) Ni/SiO₂ at 550 °C; (B) unsupported Ni catalyst at 550 °C.

The CNF produced with the gases giving the highest yields after 10 h, thus for the Ni/SiO₂ catalyst, the fibers grown out of CO/H₂ and for the unsupported Ni catalyst the CNF originating from C₂H₄/H₂ are investigated in more detail. Fig. 5 displays the SEM images of these CNF. Uniform and small diam-

eter (25 nm) CNF had been grown from CO/H₂ using the Ni/SiO₂ catalyst. In contrast to this, unsupported Ni and C₂H₄/H₂ resulted in large diameter CNF with a broad diameter distribution (50–500 nm). XRD showed that both types of CNF consisted of graphitic carbon.

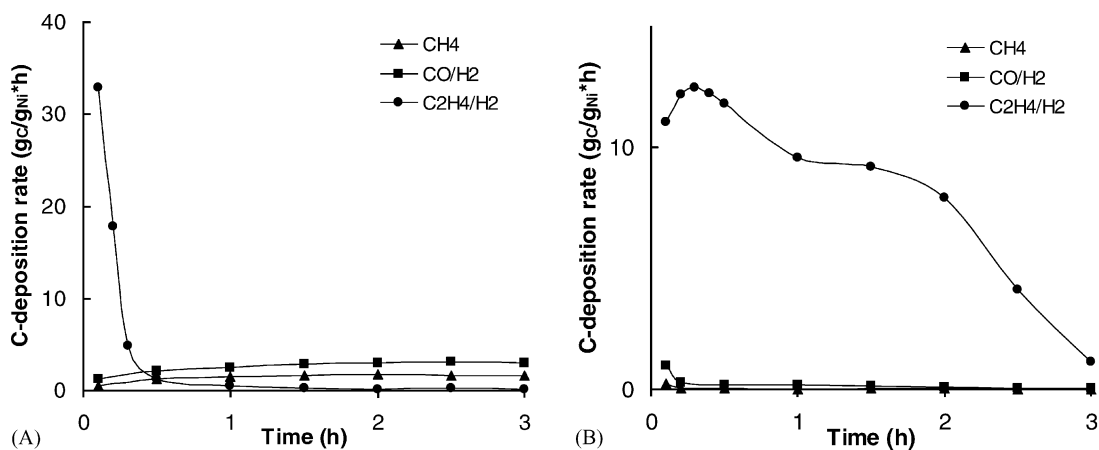


Fig. 4. Conversion of different carbon sources with a flow of 20 ml/min (total flow 100 ml/min) at 550 °C and 1 bar over (A) Ni/SiO₂ and (B) unsupported Ni.

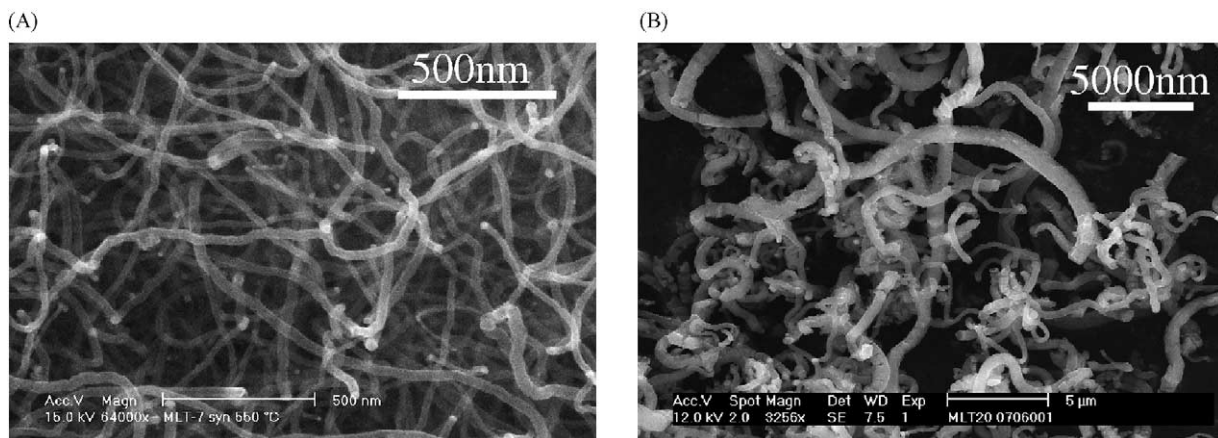


Fig. 5. SEM: (A) CNF grown using Ni/SiO₂ and 20% CO/7% H₂ at 550 °C; (B) CNF produced by unsupported Ni catalyst and 20% C₂H₄/7% H₂ at 550 °C.

Table 1

Some physico-chemical features of CNF grown at 550 °C from Ni/SiO₂, 20% CO/7% H₂ and unsupported Ni catalyst, 20% C₂H₄/7% H₂

	S_{BET} (m ² /g)	V_{micro} (ml/g)	V_{meso} (ml/g)	d_{pore} (nm)
CNF (Ni/SiO ₂ , CO/H ₂)	214	0.01	0.41	10
CNF (Ni, C ₂ H ₄ /H ₂)	54	0.01	0.10	70

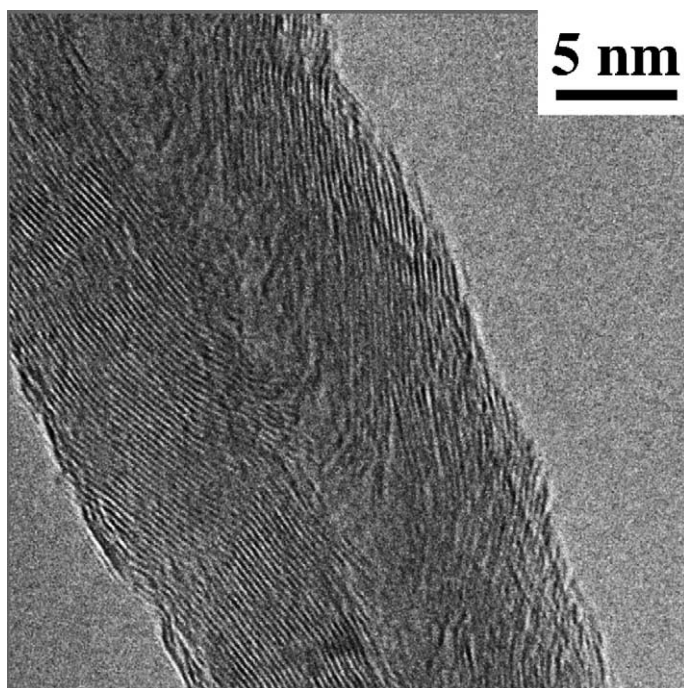


Fig. 6. TEM image of CNF grown using Ni/SiO₂ and 20% CO/7% H₂ at 550 °C.

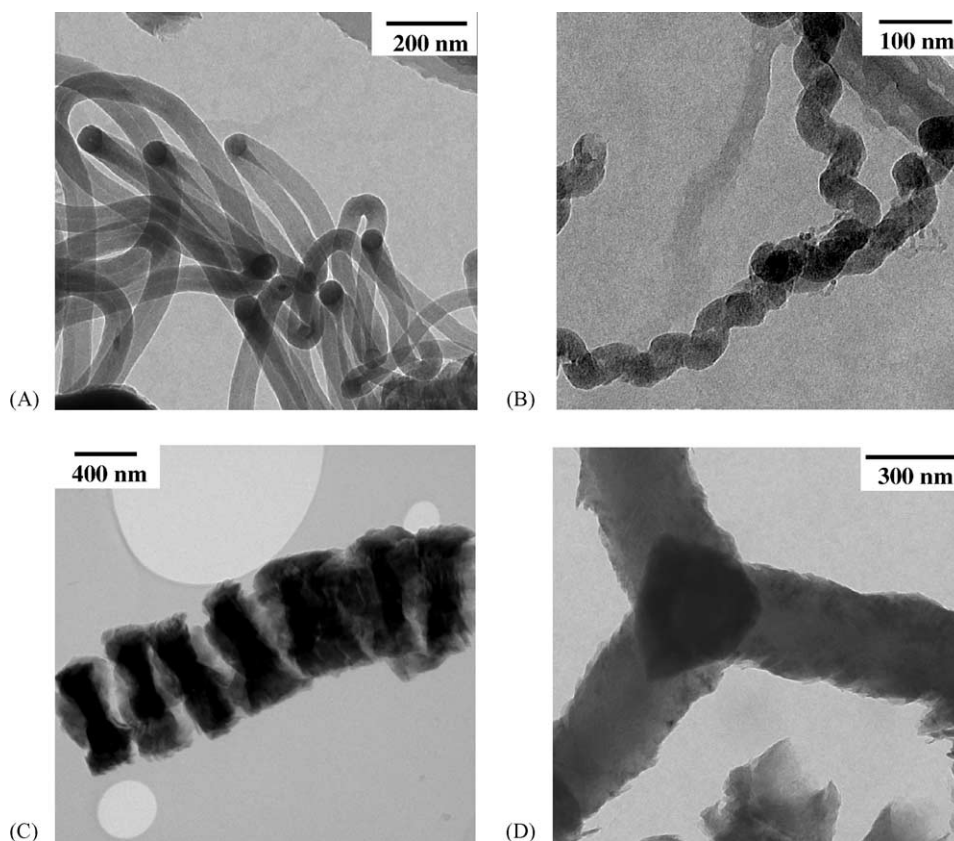


Fig. 7. (A)–(D) TEM images of CNF produced by unsupported Ni and 20% C₂H₄/7% H₂ at 550 °C.

The textural properties of both types of CNF were investigated by means of nitrogen physisorption. The results are summarized in Table 1. The small diameter CNF exhibited a high specific surface area (214 m²/g) and a high mesopore volume (0.41 ml/g). The large diameter CNF, on the other hand, had a lower surface area (54 m²/g) and mesopore volume (0.10 ml/g). The pore distributions, derived from the desorption isotherm, differed for both types of CNF. The small diameter CNF had a narrow pore size distribution with an average diameter of 10 nm. A broad pore diameter distribution was found for the large diameter CNF with an average pore diameter of 70 nm. From the corresponding *t*-plots for both types a low but not negligible micropore volume of 0.01 ml/g was derived, probably originating from the surface roughness of the fibers.

TEM pictures of the CNF grown from the supported and the unsupported catalyst are presented in

Figs. 6 and 7. These pictures clearly show the difference in the diameters of the CNF. With the small diameter CNF (Fig. 6) the individual lattice planes of the graphite lattice are visibly ordered in the fishbone structure. In contrast to the small diameter CNF, the large diameter CNF are very heterogeneous. Besides fishbone type of fibers with perfect graphitic ordering, also less ordered platelet type of fibers and some helical [32,33] and multidirectional [34,35] fibers are found (Fig. 7A–D). These large diameter CNF are too thick to make acquisition of micrographs with higher magnification meaningful.

4. Discussion

The mechanism of the catalytic growth of CNF has been studied over a long period of time. Although

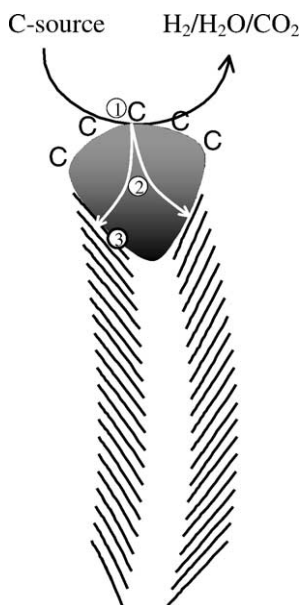


Fig. 8. Schematic representation of the catalytic growth of a CNF using a gaseous carbon-containing gas. Step 1: decomposition of carbon-containing gases on the metal surface. Step 2: carbon atoms dissolve in and diffuse through the bulk of the metal. Step 3: precipitation of carbon in the form of a CNF consisting of graphite.

consensus has been reached with respect to the different growth steps [3], still uncertainties exist about some details. A schematic representation of the mechanism of steady-state growth is given in Fig. 8 and is based on the review of de Jong and Geus [3]. The first step is the decomposition of carbon-containing gases on the metal surface. In this process carbon atoms are deposited on the surface with the concomitant release of gaseous products like molecular hydrogen, carbon dioxide and water depending on the carbon-containing gas used. In the second step the carbon atoms dissolve in and diffuse through the bulk of the metal particle, although some contribution of surface diffusion cannot be excluded. The final step is the precipitation of the carbon in the form of a CNF consisting of graphite at the other side of the metal particle. The thermodynamic driving force of the CNF production is the formation of graphite out of carbon-containing gas. The above mentioned steps show that the steady state growth process is a delicate balance between the dissociation of the carbon-containing gases, carbon diffusion through the particle, and the

rate of nucleation and formation of graphitic layers [3,20].

Addition of hydrogen is required when C_2H_4 and CO is used to balance the amount of carbon atoms in the CNF growth process. Hydrogen reduces the amount of carbon atoms formed and can therefore prevent encapsulation and thus deactivation of the catalyst.

Our study clearly demonstrates, see Figs. 3 and 4, that the CNF yield within a certain period of time strongly depends on the type of catalyst as well as on the nature of the carbon-containing gas. From the small supported nickel particles large amounts of CNF are grown from CH_4 and from CO/H_2 at an almost constant, moderate rate over the entire period of 10 h.

As already mentioned above, the mechanism of CNF growth is a delicate process. When the balance between dissociation, diffusion and segregation is disturbed, the CNF growth stops. Since with the Ni/SiO_2 catalyst and C_2H_4/H_2 a high initial rate is observed followed by fast deactivation, we have to conclude that the diffusion of the C-atoms through the metal particle and the fiber formation cannot keep up with the C-atom supply at the surface, resulting in encapsulation of the nickel particles by a layer of carbon. No clean metal surface is left to dissociate the carbon-containing gas and hence the fiber growth stops. The C-deposition rates with CH_4 and CO/H_2 are slowly increasing in the first hour, i.e. activation occurs, after which more or less a steady state is reached. This shows that with these two gases the CNF growth is a balanced process which holds for a long period of time.

With the unsupported nickel catalyst with none of the used gases a steady state production of CNF is observed. CH_4 is not converted at all, CO/H_2 shows only initially some activity, while C_2H_4/H_2 deactivates the catalyst within 3 h, notwithstanding the fact, that the activity is high and close to constant for 2 h. How to explain, to start with, the different behavior of the catalysts with respect to CH_4 and CO/H_2 ?

We are convinced that this difference originates from the difference in nickel particle size, and with this, with the different types of lattice planes exposed. From literature it is well known that the type of exposed lattice plane significantly affects the rate of hydrocarbon decomposition [23–26]. Because this

decomposition is the first step in the growth process of the fiber too, this must also hold for the rate of CNF growth when the rate of decomposition becomes rate determining.

It has been reported [8,21], that small particles from which CNF have been grown, usually are more or less spherical/conical, which implies that more open, high index planes are exposed. These planes are active for dissociation, even of CH_4 , the least reactive compound at 550°C . With larger particles the most stable, low-index plane(s) dominate the gas–solid interface [36,37], which means that only more reactive hydrocarbons, like C_2H_4 , are dissociated.

With the small nickel particles we found with $\text{C}_2\text{H}_4/\text{H}_2$ a rather high initial carbon deposition rate, which was rapidly followed by deactivation due to encapsulation. This initial rate is much higher indeed than those measured with CH_4 and CO/H_2 , probably due to the high reactivity of C_2H_4 . As we stated earlier, ultimately nucleation and fiber formation cannot keep up with the rate of hydrocarbon dissociation, due to which encapsulation occurs.

With the large, unsupported particles, however, we observed that the growth process remained for even 2 h at a surprisingly high level. From Fig. 1 we concluded that the nickel particles of the unsupported catalyst are sized in the range of 50–1000 nm but are conglomerated to even much larger units. Furthermore, XRD results make it even questionable whether the smallest particles as observed were monocrystalline. Undoubtedly, from the start of the process, carbon is deposited on all exposed surfaces, which rapidly diffuses into the bulk. Probably from the smallest particles of the conglomerates fibers start to grow because of these units diffusion paths are the shortest.

In Fig. 7A a bundle of fibers is shown with diameters of about 50 nm, a size close to that, formed from the small supported nickel particles. Striking is the observation that from each of these particles a pair of fibers had formed. Such a phenomenon we never have observed with the small particles of a supported catalyst.

A tentative explanation of the deviating behavior of the 50 nm particles is that the particles consist of two monocrystalline units, from each of which a fiber has grown. Probably these nickel particles had been expelled from the conglomerated units because of stress forces brought about by dissolution of large amounts

of carbon. It is very well possible that, if nucleation of the fibers occurred close to each other, e.g. on both sides of the interface between the monocrystalline regions, defects in the graphitic layers became introduced, which caused the helical growth [32,33] of the fibers, see Fig. 7B.

With SEM no large metal conglomerates could be found after CNF growth, only small metal fragments are observed. Obviously the process of fragmentation and the continuous formation of fresh metal surfaces is the explanation for the relatively long period of time the growth of fibers could continue. Only after 2 h the growth rate decreased and only after 3 h no fresh surfaces were formed anymore and termination of the fiber formation occurred.

The explanations given above may also hold for the formation of the multidirectional fibers [34,35] as shown in Fig. 7D. Only in this case the nickel particle is much larger and probably consist of at least several monocrystalline domains. The formed graphitic planes probably originate from more than one monocrystalline region, due to which many defects are build in, causing the variable diameter and roughness of the fibers.

The most peculiar type of fiber is shown in Fig. 7C. The thickness of the fiber, about 700 nm, indicates that in this case it must have grown from a highly polycrystalline surface from which nucleation and piling up of the layers took place rather irregularly. Possibly a pulse-like change of layer orientation and variation in fiber diameter occurred.

5. Conclusions

In this study we have demonstrated that a continuous production of CNF only is possible when carbon deposition, diffusion, nucleation and growth are in a subtle balance. This only was achieved with the small nickel particles of the supported catalyst in combination with a carbon-containing gas with a relatively low inclination for dissociation, i.e. CH_4 and CO/H_2 at 550°C . The small metal particles expose high index planes, which avoid termination of the growth process. With the more reactive $\text{C}_2\text{H}_4/\text{H}_2$ mixture, diffusion of carbon and nucleation cannot keep up with the carbon deposition due to which encapsulation rapidly terminates the growth process.

With the unsupported nickel particles termination in case of C_2H_4/H_2 is delayed due to formation of fresh metal surfaces as a result of fragmentation of the large conglomerates. A variety of fiber types is formed of which only the fibers grown from the small particles are more or less regular. Because most of the particles are large, low-index planes, incapable of dissociation of CH_4 and CO/H_2 , dominate the gas–metal interface and fiber formation is not possible at the chosen conditions.

Acknowledgements

These investigations are supported by the Council for Chemical Sciences of the Netherlands Organization for Scientific Research with financial aid from The Netherlands Technology Foundation (CW/STW 349-5357).

References

- [1] N.M. Rodriquez, J. Mater. Res. 8 (1993) 3233.
- [2] R.T.K. Baker, Carbon 27 (1989) 315.
- [3] K.P. de Jong, J.W. Geus, Catal. Rev.-Sci. Eng. 42 (2000) 481.
- [4] A. Thess, R. Lee, P. Nikolaev, H.J. Dai, P. Petit, J. Robert, C.H. Xu, Y.H. Lee, S.G. Kim, A.G. Rinzler, D.T. Colbert, G.E. Scuseria, D. Tomanek, J.E. Fischer, R.E. Smalley, Science 273 (1996) 483.
- [5] S. Iijima, Nature 354 (1991) 56.
- [6] T.W. Ebbesen, P.M. Ajayan, Nature 358 (1992) 220.
- [7] N.M. Rodriquez, M.-S. Kim, R.T.K. Baker, J. Phys. Chem. 98 (1994) 13108.
- [8] J.W. Geus, A.J. van Dillen, M.S. Hoogenraad, Mater. Res. Soc. Symp. Proc. 368 (1995) 87.
- [9] R.T.K. Baker, in: J.L. Figueiredo, C.A. Bernadro, R.T.K. Baker, K.J. Hüttinger (Eds.), Carbon Fibers, Filaments and Composites, NATO ASI Series, Kluwer Academic Publishers, Dordrecht, 1990, p. 405.
- [10] D.L. Trimm, Catal. Rev.-Sci. Eng. 16 (1977) 155.
- [11] F. Coloma, A. Sepúlveda-Escribano, J.L.G. Fierro, F. Rodríguez-Reinoso, Appl. Catal. A: Gen. 150 (1997) 165.
- [12] B. Bachiller-Baeza, A. Guerrero-Ruiz, I. Rodríguez-Ramos, Appl. Catal. A: Gen. 192 (2000) 289.
- [13] A. Giroir-Fendler, D. Richard, P. Gallezot, Stud. Surf. Sci. Catal. 41 (1988) 171.
- [14] C. Pham-Huu, N. Keller, G. Ehret, L.J. Charbonniere, R. Ziesel, M.J. Ledoux, J. Mol. Catal. A: Chem. 170 (2001) 155.
- [15] P. Gallezot, D. Richard, Catal. Rev.-Sci. Eng. 40 (1998) 81.
- [16] N.M. Rodriquez, A. Chambers, R.T.K. Baker, Langmuir 11 (1995) 3862.
- [17] A. Chambers, T. Nemes, N.M. Rodriquez, R.T.K. Baker, J. Phys. Chem. B 102 (1998) 2251.
- [18] J.-F. Colomer, P. Piedigrosso, I. Willems, C. Cournet, P. Bernier, G. Van Tendeloo, A. Fonseca, J.B. Nagy, J. Chem. Soc., Faraday Trans. 94 (1998) 3753.
- [19] P. Chen, H.-B. Zhang, G.-D. Lin, Q. Hong, K.R. Tsai, Carbon 35 (1997) 1495.
- [20] M.S. Hoogenraad, Ph.D. Thesis, Utrecht University, 1995.
- [21] E. Boellaard, P.K. de Bokx, A.J.H.M. Kock, J.W. Geus, J. Catal. 96 (1985) 481.
- [22] R.T.K. Baker, M.S. Kim, A. Chambers, C. Park, N.M. Rodriquez, Stud. Surf. Sci. Catal. 111 (1997) 99.
- [23] I. Alstrup, J. Catal. 109 (1988) 241.
- [24] M. Audier, A. Oberlin, M. Coulon, J. Crystal Growth 55 (1981) 549.
- [25] F.C. Schouten, E.W. Kaleveld, G.A. Bootsma, Surf. Sci. 63 (1977) 460.
- [26] F.C. Schouten, O.L.J. Gijzeman, G.A. Bootsma, Surf. Sci. 87 (1979) 460.
- [27] M.-S. Kim, N.M. Rodriquez, R.T.K. Baker, Mater. Res. Soc. Symp. Proc. 368 (1995) 99.
- [28] C. Menini, C. Park, R. Brydson, M.A. Keane, J. Phys. Chem. B 104 (2000) 4281.
- [29] C.D. Tan, R.T.K. Baker, Catal. Today 63 (2000) 3.
- [30] A.J. van Dillen, J.W. Geus, L.A.M. Hermans, J. van der Meijden, in: Proceedings of the Sixth International Congress, Catalysis 2 (1977) 677.
- [31] L.A.M. Hermans, J.W. Geus, Stud. Surf. Sci. Catal. 3 (1979) 113.
- [32] M.S. Kim, N.M. Rodriquez, R.T.K. Baker, J. Catal. 134 (1991) 253.
- [33] S. Amelinckx, X.B. Zhang, D. Bernaerts, X.F. Zhang, V. Ivanov, J.B. Nagy, Science 265 (1994) 635.
- [34] M.T. Tavares, C. Bernardo, I. Alstrup, J.R. Rostrup-Nielsen, J. Catal. 100 (1986) 545.
- [35] H. Terrones, T. Hayashi, M. Munoz-Navia, M. Terrones, Y.A. Kim, N. Grobert, R. Kamalakaran, J. Dorantes-Davila, R. Escudero, M.S. Dresselhaus, M. Endo, Chem. Phys. Lett. 343 (2001) 241.
- [36] N.M. Rodriquez, in: Kuzmany, Fink, Mehring, Roth, (Eds.), Proceedings of the International Wintersch. Electron. Prop. Novel Mater. on Mol. Nanostruct., World Scientific Publishing Company, 1998, p. 495.
- [37] V.I. Zaikovskii, V.V. Chesnokov, R.A. Buyanov, Appl. Catal. 38 (1988) 41.